

## CMMB Primary User Detection based on Data Smoothing using Scattered Pilots in Cognitive Radio

<sup>1</sup>Huiheng Liu, <sup>2</sup>Yuanyuan Yang and <sup>3</sup>Wei Chen  
<sup>3</sup>Member, IEEE

<sup>1</sup> School of Physics and Electronic Engineering, Hubei University of Arts and Science, Xiangyang 441053, China

<sup>2,3</sup> School of Information Engineering, Wuhan University of Technology, Wuhan 430070, China

<sup>1</sup> lhh117@163.com, <sup>2</sup> yangyuanyuan@whut.edu.cn, <sup>3</sup> greatchen@whut.edu.cn

### Abstract

The cyclostationarity of China multimedia mobile broadcasting (CMMB) signal is explored. A low-complexity detection algorithm in cognitive radio for the CMMB primary user based on data smoothing using scattered pilots is proposed. First, the received data in the secondary user is smoothed by the first order lag filter. Then some special delay lags are selected to calculate the cyclic autocorrelation function (CAF) as a decision statistic. When the cycle frequency is equal to zero, some dominant peaks of scattered pilots will appear in CAF for the special delay lags. Fully considering the cyclostationary feature mentioned above, these peaks are used to detect the CMMB primary user. Simulation results show that the proposed algorithm has a good detection performance, especially under long sensing time conditions.

**Keywords:** data smoothing; scattered pilots; cyclic autocorrelation function; CMMB; cognitive radio

### 1. Introduction

Cognitive radio has emerged as a potential technology to improve the spectrum utilization and solve the spectrum scarcity problem [1]. As a fundamental and key issue in cognitive radio, spectrum sensing has been explored comprehensively [2-4]. There are basically two spectrum sensing methods: narrowband sensing and wideband sensing. In practice, due to either the high implementation complexity or high financial/energy costs, the wideband sensing schemes are difficult to design [5]. The narrowband sensing methods can be classified into energy detection (ED), matched filter detection and cyclostationary feature detection (CFD). Among them, the CFD method can effectively distinguish the signal and noise, which is robust to the noise uncertainty. Although it has the high computational complexity, the CFD method is frequently used for the spectrum sensing, especially for some signals with the cyclostationary feature, *i.e.* orthogonal frequency division multiplexing (OFDM), which is the most popular modulation scheme in the communication and broadcasting systems, such as digital video broadcasting - terrestrial (DVB-T), worldwide interoperability for microwave access (WiMax), long term evolution (LTE) and China multimedia mobile broadcasting (CMMB) [6]. CMMB is a mobile television and multimedia standard developed and used by China. It provides broadcasting and television services for mobile phones, iPad and other small screen portable terminals using an S-band satellite.

Most of the existing OFDM spectrum sensing methods make use of the cyclic prefix (CP) or cyclostationarity of OFDM signals [7]. Spectrum sensing for the signal with the cyclostationarity is usually realized by calculating its cyclic autocorrelation function

(CAF). The detection methods using multiple cyclic frequencies were presented in [8], which are based on the second-order cyclic cumulants form of the CFD method. Furthermore, in order to reduce the amount of transmitted data, a censoring cooperative detection scheme also was proposed in [8], which can achieve almost the same detection performance compared with the cooperative scheme. The hard and soft decision combining cooperative detection schemes of the CFD method were analyzed in [9]. These detection schemes can achieve better detection performance, but suffer from the high complexity. However, for some OFDM signals embedded with pilot signals, *i.e.* CMMB, it is possible to reduce the complexity of the CFD method by calculating CAF positioned in the specified delay lags. Hence, a low-complexity detection algorithm of the CMMB primary user employing scattered pilots is proposed based on data smoothing in cognitive radio. According to the position of scattered pilots, some special delay lags, approximately  $\tau = nT_u/4$  where  $n=1, 2, 3$ ,  $T_u$  is the used time of an OFDM symbol of the CMMB signal, are selected to compute the decision static, CAF, with the cycle frequency  $\alpha = 0$ . The proposed algorithm has a lower complexity than the detection methods of the second-order or higher orders cyclic cumulants form. It has a better detection performance as well with fully considering the cyclostationary feature of the CMMB primary user.

## 2. Signal Feature of CMMB Primary User

Depending on the data rate, the channel bandwidth of a CMMB system can be either 2 or 8 MHz. A CMMB frame consists of 40 time slots, and the length is 25ms. Each time slot consists of one beacon signal and 53 OFDM symbols. The OFDM symbol of CMMB is modulated with BPSK, QPSK, QAM16 or QAM64, in which the length of cyclic prefix is 1/8 of the data length.

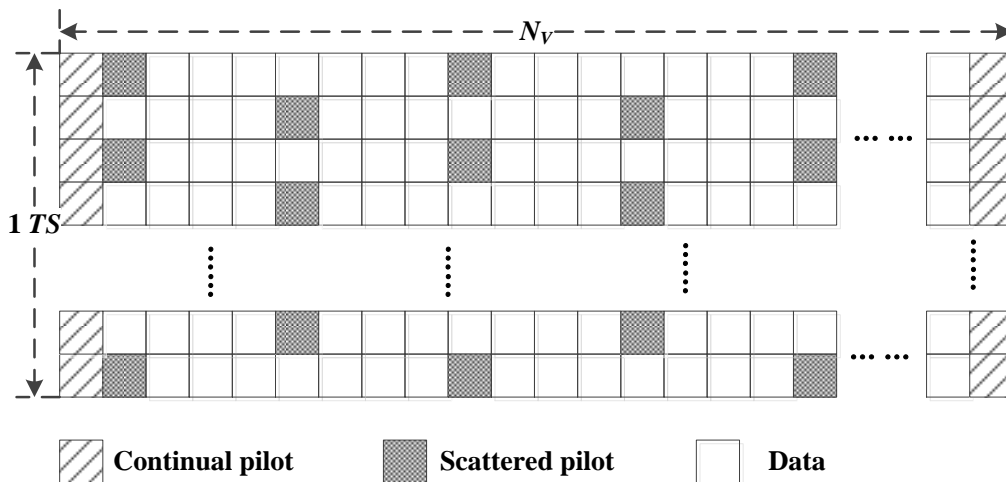


**Figure 1. The Subcarrier Positions of Continual Pilots, Scattered Pilots and Data of the CMMB signal in One Time Slot (1TS)**

In order to aid the channel estimation and synchronization, the CMMB system inserts pilot signals with a regular repeat. As shown in Figure 1, three types of effective subcarriers, data, scattered pilots and continual pilots, are usually set up for the CMMB signal in the frequency domain, where  $N_v$  is the number of effective subcarriers. For B=2MHz mode, the amount of data, scattered pilots and continual pilots are 522, 78 and 28, respectively. In the arrangement of configuration, the position of scattered pilot subcarriers for the CMMB signal periodically changes and is repeated every 8 subcarriers.

Furthermore, there are more scattered pilots in comparison with the continual pilots. Therefore, the scattered pilots of the CMMB primary user will generate a well-detectable signature.

If the channel bandwidth is 2MHz, the position of the  $m$ th scattered pilot in the  $n$ th OFDM symbol is as follows:

$$\begin{aligned} & \text{if } \text{mod}(n,2) = 0 \\ & m = \begin{cases} 8p+1, & p = 0,1,\dots,38 \\ 8p+3, & p = 39,40,\dots,77 \end{cases} \\ & \text{if } \text{mod}(n,2) = 1 \\ & m = \begin{cases} 8p+5, & p = 0,1,\dots,38 \\ 8p+7, & p = 39,40,\dots,77 \end{cases} \end{aligned} \quad (1)$$

### 3. Proposed Method

#### 3.1. Cyclostationarity

The process  $x(t)$  is assumed to be a second-order cyclostationary if its mean and autocorrelation function are periodic with period  $T_0$ . It can be written as

$$R_{xx}(t, \tau) = R_{xx}(t+T_0, \tau) = E \left[ x(t+\frac{\tau}{2}) x^*(t-\frac{\tau}{2}) \right] \quad (2)$$

Because of the periodicity of autocorrelation function, it can be represented by its Fourier series expansion

$$R_{xx}(t, \tau) = \sum_{\alpha} R_{xx}^{\alpha}(\tau) e^{j2\pi\alpha t} \quad (3)$$

where

$$R_{xx}^{\alpha}(\tau) = \lim_{T_0 \rightarrow \infty} \frac{1}{T_0} \int_{-\frac{T_0}{2}}^{\frac{T_0}{2}} R_{xx}(t, \tau) e^{-j2\pi\alpha t} dt \quad (4)$$

is CAF of  $x(t)$ ,  $\alpha$  is called the cycle frequency, where  $\alpha = m \frac{1}{T_0}$ , and  $m$  is a integer.

#### 3.2. System Model

The baseband of the CMMB primary user in the time domain can be expressed as

$$S(t) = \sum_{n=-\infty}^{\infty} \sum_{i=0}^{N_u-1} Z(i,n) e^{j2\pi \frac{i}{T_u} t} p(t-nT_s) \quad (5)$$

where  $n$  is the  $n$ th OFDM symbol and  $i$  is the  $i$ th subcarrier.  $Z(i,n)$  is the effective subcarriers  $N_v$  mapped to the used subcarriers  $N_u$ . The total subcarriers  $N_s = N_u + N_{cp}$  of which  $N_{cp}$  is the number of cyclic prefixes.  $T_u$  is the used time of an OFDM symbol and  $T_s = T_u + T_{cp}$  is the total time of an OFDM symbol.  $T_{cp}$  is the duration of cyclic prefix,  $p(t-nT_s)$  is a rectangular pulse function.

To determine the cyclostationary feature, the baseband OFDM signal of CMMB can be written in the form of the summation of data subcarriers and scattered pilot subcarriers defined as (6), where  $d(i,n)$  is the data information,  $a(I_1(l),n)$  and  $a(I_2(l),n)$  are the scattered pilot subcarriers, *i.e.*  $a(I_1(l),n) = a(I_2(l),n) = 1+0j$ .  $N_p = 39$  is half the pilot subcarriers of an OFDM symbol.  $I_1(l) = S_1 + L_p l, l = 0,1,\dots,N_p - 1$ , is the position of the first half of pilot subcarriers,  $S_1$  is the starting pilot subcarrier and  $L_p = 8$  is the scattered pilot interval.  $I_2(l) = S_2 + L_p l, l = N_p, N_p + 1, \dots, 2N_p - 1$ , is the position of the second half of pilot subcarriers,  $S_2$  is the starting pilot subcarrier.

$$S(t) = \sum_{n=-\infty}^{\infty} \left( \sum_{i=0, i \neq I_1(l), i \neq I_2(l)}^{N_u-1} d(i, n) e^{j2\pi \frac{i}{T_u} t} + \sum_{l=0}^{N_p-1} a(I_1(l), n) e^{j2\pi \frac{S_1+L_p l}{T_u} t} + \sum_{l=N_p}^{2N_p-1} a(I_2(l), n) e^{j2\pi \frac{S_2+L_p l}{T_u} t} \right) \cdot p(t-nT_s) \quad (6)$$

### 3.3. CMMB Primary User Detection

Let  $R_{SS}(t, \tau)$  denote CAF of different OFDM symbols of the CMMB primary user. It is given by (7).

$$R_{SS}(t, \tau) = \sum_{n=-\infty}^{\infty} \left\{ \sum_{i=0, i \neq I_1(l), i \neq I_2(l)}^{N_u-1} E[d(i, n)d^*(i, n)] e^{j2\pi \frac{i}{T_u} \tau} + \sum_{l=0}^{N_p-1} E[a(I_1(l), n)a^*(I_1(l), n)] e^{j2\pi \frac{S_1+L_p l}{T_u} \tau} + \sum_{l=N_p}^{2N_p-1} E[a(I_2(l), n)a^*(I_2(l), n)] e^{j2\pi \frac{S_2+L_p l}{T_u} \tau} \right\} \cdot p\left(t+\frac{\tau}{2}-nT_s\right) p^*\left(t-\frac{\tau}{2}-nT_s\right) \quad (7)$$

Assumed the modulated signal  $S(t)$  is independent, and identically distributed (*i.i.d.*), then  $E[d(i, n)d^*(i, n)]$  is equal to the average power  $\sigma_u^2$  of data subcarriers,  $E[a(I_1(l), n)a^*(I_1(l), n)]$  and  $E[a(I_2(l), n)a^*(I_2(l), n)]$  are equal to the average powers of the first and the second half of scattered pilot subcarriers,  $\sigma_{p1}^2$  and  $\sigma_{p2}^2$ , respectively. Then (7) is simplified to (8).

$$R_{SS}(t, \tau) = \left[ \sigma_u^2 \sum_{i=0}^{N_u-1} e^{j2\pi \frac{i}{T_u} \tau} - (\sigma_u^2 - \sigma_{p1}^2) \sum_{l=0}^{N_p-1} e^{j2\pi \frac{S_1+L_p l}{T_u} \tau} - (\sigma_u^2 - \sigma_{p2}^2) \sum_{l=N_p}^{2N_p-1} e^{j2\pi \frac{S_2+L_p l}{T_u} \tau} \right] \cdot \sum_{n=-\infty}^{\infty} p\left(t+\frac{\tau}{2}-nT_s\right) p^*\left(t-\frac{\tau}{2}-nT_s\right) \quad (8)$$

The sum terms of (8) can be simplified according to the Euler's formula. For example,

$$\sum_{i=0}^{N_u-1} e^{j2\pi \frac{i}{T_u} \tau} = \frac{1 - e^{j2\pi \frac{N_u}{T_u} \tau}}{1 - e^{j2\pi \frac{\tau}{T_u}}} = \frac{e^{j\pi \frac{N_u}{T_u} \tau} (e^{-j\pi \frac{N_u}{T_u} \tau} - e^{j\pi \frac{N_u}{T_u} \tau})}{e^{j\pi \frac{\tau}{T_u}} (e^{-j\pi \frac{\tau}{T_u}} - e^{j\pi \frac{\tau}{T_u}})} = \frac{\sin(\frac{N_u \pi \tau}{T_u})}{\sin(\frac{\pi \tau}{T_u})} \cdot e^{j\pi (N_u-1) \frac{\tau}{T_u}} \quad (9)$$

The other two sum terms can be simplified similarly.

Considering the finite representation, the Fourier coefficient of the second term in (8) is denoted by

$$R_{pp}^{\alpha}(\tau) = \frac{1}{T_s} \int_{-\frac{T_s}{2}}^{\frac{T_s}{2}} \sum_{n=-\infty}^{\infty} p\left(t+\frac{\tau}{2}-nT_s\right) p^*\left(t-\frac{\tau}{2}-nT_s\right) e^{-j2\pi \alpha t} dt \quad (10)$$

$$= \frac{1}{T_s} \int_{-\frac{T_s}{2}}^{\frac{T_s}{2}} p\left(t+\frac{\tau}{2}\right) p^*\left(t-\frac{\tau}{2}\right) e^{-j2\pi \alpha t} dt$$

where  $\alpha$  is an integer multiple of  $\frac{1}{T_s}$ . Given that  $p(t)$  is a rectangular pulse with value 1 for  $-T_s \leq t \leq T_s$  and value 0 elsewhere, if  $\tau > 0$ , we have

$$R_{pp}^{\alpha}(\tau) = \frac{1}{T_s} \int_{-\frac{T_s}{2}}^{\frac{T_s}{2}} e^{-j2\pi \alpha t} dt = \frac{\sin[\pi \alpha (T_s - \tau)]}{\pi \alpha T_s} \quad (11)$$

Similarly, if  $\tau < 0$ ,  $R_{pp}^{\alpha}(\tau)$  is equal to  $\frac{\sin[\pi \alpha (T_s + \tau)]}{\pi \alpha T_s}$ . Considering the above two cases,

$R_{pp}^{\alpha}(\tau)$  becomes

$$R_{pp}^{\alpha}(\tau) = \frac{\sin[\pi \alpha (T_s - |\tau|)]}{\pi \alpha T_s} \quad (12)$$

By substitution in the finite representation of (3), (4) and considering (9) and (12), the Fourier coefficient  $R_{SS}^\alpha(\tau)$  of  $R_{SS}(t, \tau)$  is given by (13).

$$R_{SS}^\alpha(\tau) = \left\{ \begin{array}{l} \frac{\sin(\frac{N_u \pi \tau}{T_u})}{\sin(\frac{\pi \tau}{T_u})} \cdot e^{j\pi(N_u-1)\frac{\tau}{T_u}} - \frac{\sin(\frac{N_p L_p \pi \tau}{T_u})}{\sin(\frac{L_p \pi \tau}{T_u})} \\ \left[ (\sigma_u^2 - \sigma_{p1}^2) e^{j\pi[2S_1 + L_p(N_p-1)]\frac{\tau}{T_u}} + (\sigma_u^2 - \sigma_{p2}^2) e^{j\pi[2S_2 + L_p(3N_p-1)]\frac{\tau}{T_u}} \right] \cdot \frac{\sin[\pi\alpha(T_s - |\tau|)]}{\pi\alpha T_s} \end{array} \right. \quad (13)$$

Equation (13) shows CAF of the CMMB primary user with the scattered pilot structure is influenced dominantly by the scattered pilots. It can be observed that  $R_{SS}^\alpha(\tau)$  generate peaks for  $\alpha=0$  and approximately  $\tau = n \frac{T_u}{L_p}$ ,  $n=1, 2, \dots, L_p-1$ . Indeed, the starting subcarrier of scattered pilots is different in the first and the second half of one symbol. In addition, the starting subcarrier of scattered pilots is also different for every adjacent two symbols. Therefore, only two symbols of CMMB generate some well-detectable peaks at approximately  $\tau = 2n \frac{T_u}{L_p} = n \frac{T_u}{4}$ ,  $n=1, 2, 3$ .

As shown in (13), the average powers of data subcarriers and scattered pilot subcarriers have a great influence on CAF,  $R_{SS}^\alpha(\tau)$ . The average powers are influenced by the noise. The noise can be considered as a circularly symmetric complex Gaussian (CSCG) noise in the OFDM symbols, and the first order lag filter is suitable to filter the CSCG noise. Therefore, we use it to smooth the received data. Then the average powers better reflect the actual powers of data subcarriers and scattered pilot subcarriers. Assumed the smoothed data of the  $n$ th OFDM symbol and  $i$ th subcarrier is  $\bar{S}(i, n)$ , we have

$$\bar{S}(i, n) = (1-b) \cdot S(i, n) + b \cdot \bar{S}(i-1, n), \quad b \in (0, 1) \quad (14)$$

where  $S(i, n)$  is the signal interfered with the noise,  $\bar{S}(i-1, n)$  is the smoothed data in last calculation, and  $b$  is the smoothing factor.

Hence, the decision rule is denoted by

$$\begin{cases} H_1 : \bar{R}_{SS}^\alpha(\tau) \geq \lambda \\ H_0 : \bar{R}_{SS}^\alpha(\tau) < \lambda \end{cases} \quad (15)$$

where  $\bar{R}_{SS}^\alpha(\tau)$  is CAF of (13), where the average powers of the data and scattered pilot subcarriers are computed with the smoothed data,  $\lambda$  is the decision threshold. For a target probability of false alarm,  $\lambda$  is obtained by Monte Carlo simulation with only if the noise existence.

### 3.4. Complexity

The complexity of the proposed algorithm in case of the number of multiplications can be expressed in terms of  $O(MN_s)$ , where  $M$  is the number of OFDM symbols used for the spectrum sensing. The proposed algorithm has a lower complexity than the second-order cyclic cumulants form using multiple cycle frequencies with the same one delay lag, which is denoted by  $O(M \cdot (LN_s^2 + N_s \log N_s))$ , where  $L$  is the odd length of a spectral window. Even considering one cyclic frequency, the form of second-order cyclic cumulants still has a higher complexity with  $O(M \cdot (LN_s + N_s))$ .

#### 4. Simulation Results

In this section, we provide some simulation results for the CM-MB primary user with the bandwidth  $B=2\text{MHz}$  average on 2000 Monte Carlo realizations. The subcarrier modulation is QAM16, although we can get similar results with other mapping schemes, such as BPSK, QPSK or QAM64. The special delay lag  $\tau$  is set to  $T_u/4$ . Obviously, the bigger the value of the smoothing factor  $b$ , the smoothing effect is better of  $\bar{S}(i,n)$  in (14). Hence, the smoothing factor  $b=0.99$  is set for all simulations.

Figure 2 depicts the detection performances for the CM-MB primary user in AWGN and frequency selective Rayleigh fading channels. The number of OFDM symbols used for the spectrum sensing is  $M=108$ , it is equal to two slot times (50ms) of a CM-MB frame. The parameters of the CM-MB primary user are as follows:  $N_u = 1024$ ,  $N_v = 628$ ,  $N_{cp} = 128$ . The sampling rate is 20MHz. The same simulation parameters,  $N_u$ ,  $N_v$ ,  $N_{cp}$  and the sampling rate, are used in the following simulation as well. It can be observed that the probability of detection goes up with the probability of false alarm increasing. In AWGN channel, when the SNR is bigger, *i.e.*  $\text{SNR} \geq -8\text{dB}$ , the detection probability of the proposed scheme is up to 1. In order to evaluate the effect of data smoothing, the detection performance without data smoothing for the target probability of false alarm  $P_f = 0.05$  is also simulated in AWGN channel. It can be seen that the performance with data smoothing is improved greatly. In addition, the detection performance of the proposed algorithm is a little worse in frequency selective Rayleigh fading channel than in AWGN channel. The performance degradation is about 2-3dB which shows that the robustness of the proposed algorithm both in AWGN and Rayleigh channels.

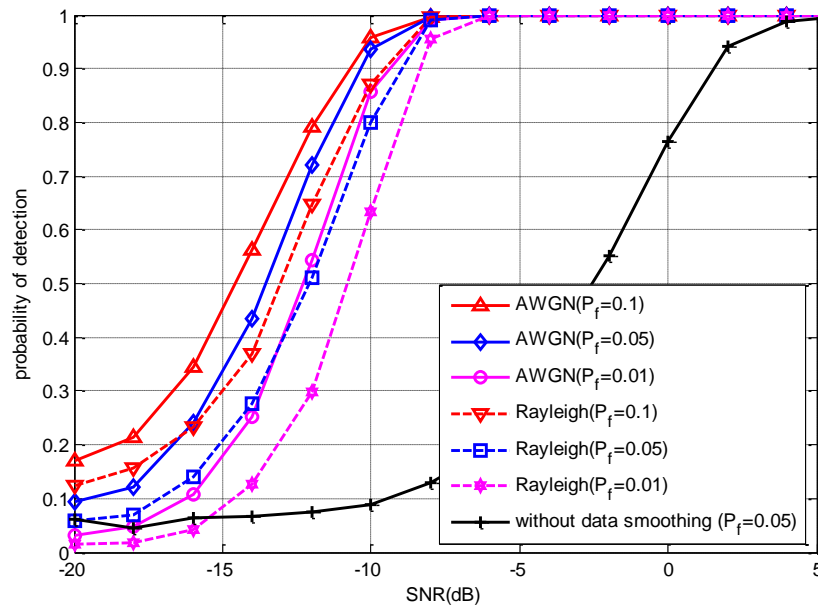


**Figure 2. The Detection Performance of the Proposed Algorithm in AWGN and Frequency Selective Rayleigh Fading Channels**

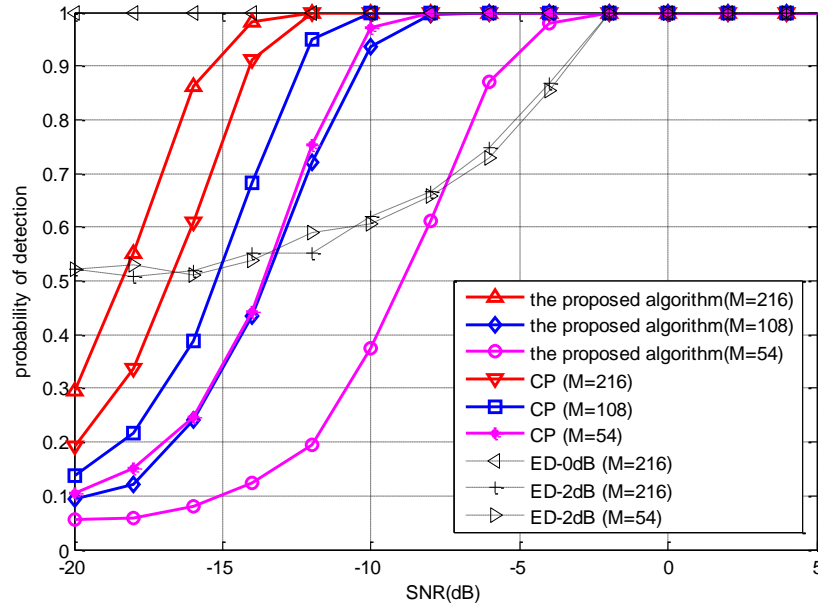


**Figure 3. The Detection Performances of the proposed Algorithm, ED and CP Methods**

Figure 3 shows the results of the proposed algorithm, the CP method in [7] and the ED scheme in AWGN channel. The target probability of false alarm  $P_f$  is 0.05. The sensing time of 25ms, 50ms, and 100ms are used, which are equal to the number of OFDM symbols  $M=54$ , 108 and 216, respectively. In fact, due to the noise uncertainty, the estimated noise power may be different from the actual noise power for the ED method. We define the estimated noise power is  $\hat{\sigma}_n^2 = \delta\sigma_n^2$ , where  $\sigma_n^2$  is the actual noise power and  $\delta$  is the noise uncertainty factor. The noise uncertainty factor  $\delta$  (in dB) follows a uniform distribution in  $[-A A]$ , and  $A$  is the upper bound of  $\delta$ , that is  $A = \max\{10\log_{10} \delta\}$ . Actually, the noise uncertainty upper bound of receiving device is normal 1 to 2dB. So in the following simulation, we choose  $\delta$  equal to 0dB, 1dB and 2dB, which are denoted by ED-0dB, ED-1dB and ED-2dB, respectively, where ED-0dB denotes that the noise power is known.

It can be verified that the detection probability of the proposed method improves significantly with the sensing time increasing. The reason originates from more scattered pilots with a long detection time. Therefore the cyclostationarity of scattered pilots is more obvious. When the sensing time is short (*e.g.*  $M=54$ , 108), the detection performance of the CP method outperforms over the proposed method. However, the proposed method exhibits a better detection performance with a longer detection time. As shown in Figure 3, under low SNR surroundings, the performance improvement is about 2-4dB compared with the CP method when the sensing time is 100ms. Furthermore, the complexity of the CP method in case of the number of multiplications,  $O(N_{cp} \cdot (MN_s))$ , is  $N_{cp}$  times the proposed scheme. On the other hand, if the noise power is known, the detection performance of the ED method is the best. In fact, the noise power is unknown, and then the performance of the ED method will be degraded. Moreover, it would not be improved with the sensing time increasing.

## 5. Conclusions

The CFD method is frequently used for the spectrum sensing in cognitive radio. Considering the cyclostationary feature of the CMMB primary user, a simple and effective spectrum sensing method is proposed in this paper. We use the first order lag filter to smooth the received data in secondary user to reduce the influence of CSCG noise. Then the value of CAF in some specified delay lags is computed directly to detect the CMMB primary user. Simulation results show that the proposed method is robust both in AWGN and Rayleigh channels. When it is compared to the CP method, the proposed method outperforms the CP method for a long sensing time. At the same time, it has a lower complexity than the second-order or higher order cyclic cumulants form detection schemes based on the CFD method. The proposed scheme is an independent detection method. However, independent detection will be degraded because of the problems of fading, shadowing and hidden terminals. In the future research, we are ready to explore the cooperative spectrum sensing method using CMMB signal feature to improve the sensing performance.

## Acknowledgements

This work was supported by the Foundation of Education Department of Hubei Province, China (No. D20162603).

## References

- [1] J. Mitola and G. Q. Maguire, "Cognitive radio: making software radios more personal", *IEEE Personal Communications*, vol.6, (1999), pp.13-18.
- [2] H. Sun, C. Wang and Y. Chen, "Wideband spectrum sensing for cognitive radio networks: a survey", *IEEE Wireless Communications*, vol. 20, (2013), pp. 74-81.
- [3] T. Yucek and H. Arslan, "A survey of spectrum sensing algorithms for cognitive radio applications", *IEEE Communication Surveys and Tutorials*, vol. 11, (2009), pp. 116-130.
- [4] F. Akyildiz, B. F. Lo and R. Balakrishnan, "Cooperative spectrum sensing in cognitive radio networks: A survey", *Physical Communication*, vol. 4, (2011), pp. 40-62.
- [5] H. Ekram and V. K. Bhargava, "Cognitive Wireless Communications Networks", Springer-Verlag New York Inc., (2007).
- [6] [Y/T 220.1-2006, "Mobile Multimedia Broadcasting Part 1: Frame Structure, Channel Coding and Modulation for Broadcasting Channel", Chinese Standard of Radio, Film and Television industry, (2006) (in Chinese).
- [7] S. Chaudhari, J. Lunden and V. Koivunen, "Collaborative Autocorrelation-based spectrum sensing of OFDM signals in cognitive radios", 42nd Annual Conference on Information Sciences and Systems, Princeton, NJ, USA, (2008), pp. 191-196.
- [8] J. Lunden, V. Koivunen, A. Huttunen and H. V. Poor, "Collaborative cyclostationary spectrum sensing for cognitive radio systems", *IEEE Transactions on Signal Processing*, vol. 57, (2009), pp. 4182-4195.
- [9] H. Sadeghi and P. Azmi, "Cyclostationarity-based cooperative spectrum sensing for cognitive radio networks", 2008 International Symposium on Telecommunications, Tehran, Iran, (2008), pp. 429-434.

## Author



**Huiheng Liu**, he received his B.S. degree in communication engineering, the M.S. degree in communication and information system, and the PhD degree in information and communication engineering from Wuhan University of Technology, China, in 2002, 2005 and 2014, respectively. Now, he is an associate professor in the School of Physics and Electronic Engineering, Hubei University of Arts and Science. His research interests include wireless communication, cognitive radio network and computer communication.